Power law indentation creep of Sn-5% Sb solder alloy

A. R. GERANMAYEH
Department of Mechanical Engineering, Azad University, South Tehran Branch, Tehran, Iran
R. MAHMUDI*
Department of Metallurgical and Materials Engineering, Faculty of Engineering, University of Tehran, P.O. Box 11365-4563, Tehran, Iran
E-mail: mahmudi@ut.ac.ir

Creep behavior of the lead-free Sn-5%Sb solder alloy was studied by long time Vickers indentation testing at room temperature. Based on the steady-state power law creep relationship, the stress exponents were determined for the cast and wrought materials in the homogenized and unhomogenized conditions. The stress exponent values of 4.5 and 12, depending on the processing route of the material, are in good agreement with those reported for the same material in conventional creep testing at room temperature. The results are discussed on the basis of the microstructural features developed during different processing routes of the material.

1. Introduction

Tin-antimony alloys are considered as suitable candidates for lead-containing solders the application of which has been restricted due to their environmental problems. One of these materials used as solders in electronic packaging is the near-peritectic composition, Sn-5%Sb, with a relatively high melting point of 245°C and a solder-substrate contact angle of about 43° [1, 2]. Low cycle fatigue, resulting from differences in coefficient of thermal expansion between components connected by solder joints, is a prime cause of joint failure in electronic industry [3]. In these fatigue processes, however, creep mechanisms play an important role because of the high homologous temperatures involved. Furthermore, in some applications, such as optical interconnects, dimensionally stable solders are needed because any creep deformation may result in a device failure [4]. Therefore, the creep study of tin-antimony alloys has received a great deal of attention [1, 2, 5, 6]. The general conclusion is that while antimony atoms in solution have only a minor effect on the creep resistance, alloys with higher concentrations of antimony contain cuboid and whisker type SnSb precipitates which provide a significant composite strengthening effect that reduces the creep rate of the material especially at temperatures below 100°C.

Several papers have addressed the possibility of gaining information on creep properties by the use of indentation or long time hardness tests [7–10]. When a constant load is applied on the surface of a sample with a suitable indenter over a period of time, plastic yield and creep take place as the indenter penetrates the material. The variation in the indentation size, expressed either as a change in diameter (Brinell test) or diagonal length (Vickers test) is monitored with dwell time. Thus, the time-dependent flow behavior of materials can be studied by these simple hardness tests. This can be particularly advantageous when the material is only available as small test-pieces or there are some difficulties with the machining of samples made of very soft materials. Therefore, the indentation creep tests, regarded as a quick, simple and non-destructive procedure to extract information on the mechanical behavior of materials, not only greatly reduce the effort for sample preparation but also reduce the sample-to-sample variation in properties [11, 12].

2. Analysis of indentation creep

It is generally accepted that the mechanical behavior of metallic materials at homologous temperatures higher than 0.5 can be fairly expressed by the power-law creep in a wide range of strain rates [13–16]. Thus, for steady-state creep, the relationship between the strain rate, $\dot{\varepsilon}$, and the tensile stress, σ, at a constant temperature can be expressed by:

$$\dot{\varepsilon} = B\sigma^n \quad (1)$$

where n is the stress exponent and B is a constant.

In an indentation test the load F on the indenter is carried by a projected indent area A, so that the indentation pressure is $H = F/A$. It creates a stress field below the indenter. For equilibrium, each component of stress in the material is proportional to F/A, so the

*Author to whom all correspondence should be addressed.

applied stress at each point beneath the indenter is given by:

$$\sigma = C\frac{F}{d^2} \tag{2}$$

where C is a constant and d is the average diagonal length. Substituting Equation 2 into Equation 1 gives:

$$\dot{\varepsilon} = K_1\left(\frac{F}{d^2}\right)^n \tag{3}$$

where K_1 is a constant. In the indentation experiments the strains are not uniform, however, the earlier experimental results show that the hardness behavior is consistent with the assumption that there is a representative strain that is simply a linear function of d [17]. Thus, at any stage in the indentation process:

$$\dot{\varepsilon} = K\dot{d} \tag{4}$$

where $\dot{d}$ is the rate of indentation length variation with time and K is a constant. Substituting Equation 4 into Equation 3, $\dot{d}$ can be expressed as:

$$\dot{d} = A_1\left(\frac{F}{d^2}\right)^n \tag{5}$$

The integration of this differential equation yields to an expression of the following form:

$$\frac{d^{2n+1}}{2n+1} = A_1F^nt + K_2 \tag{6}$$

This equation can be further simplified to a power law function:

$$d = At^b + K_3 \tag{7}$$

where K_3 is a constant, A is a constant depending on the temperature and the applied load and b is a time exponent which is inversely proportional to the stress exponent defined as:

$$b = \frac{1}{2n+1} \tag{8}$$

Rearranging for n, the stress exponent can be calculated as:

$$n = \frac{1-b}{2\text{b}} \tag{9}$$

Therefore, by plotting indentation length against time and obtaining b and n values, it is possible to study the creep behavior of materials. The aim of this paper is to investigate the indentation creep behavior of cast and wrought Sn-5%Sb alloys at room temperature, which is about a homologous temperature of 0.57 for these alloys.

3. Experimental procedure

3.1. Materials and processing

The material used was an Sn-Sb alloy containing 5 wt.% Sb. It was prepared from high purity tin (99.99%) and an Sn-20%Sb master alloy melted in an electrical furnace under inert argon atmosphere, and cast into $120 \times 30 \times 12$ mm slabs. To study the effect of homogenization on the creep behavior of the material, some of the slabs were homogenized for 24 h at 505 K. Some of the homogenized and unhomogenized cast slabs were cut into $2 \times 30 \times 12$ mm slices using an electrodischarge wire cut machine and some others were rolled to a 83% reduction at room temperature ($T > 0.5T_m$) in order to generate a homogeneous fine grained material without the initial as cast structure. Homogenized and unhomogenized conditions are referred to hereafter as "H" and "U", respectively, followed by "C" for the cast and "W" for the wrought materials. Both cast and wrought conditions were studied by optical microscopy to examine the microstructure evolution of the materials. The specimens were polished with 0.25 μm diamond paste, followed by polishing on a microcloth without any abrasive. Etching was carried out using a 2% nitric acid and 98% alcohol solution at room temperature. The structure of the materials was thus revealed and the average grain size was measured by the grain count method.

3.2. Indentation creep tests

The polished specimens were tested in a Vickers hardness tester where the applied load and testing time were the only variables. In the Vickers test, a diamond pyramid with square base is used and the Vickers hardness number is given by $H_v = 0.185F/d^2$, where F is the applied load in N and d is the average diagonal length in mm. Indentation creep measurements were made on each sample using loads of 20, 30, 50 and 100 $N$for dwell times up to 120 min. Each reading was an average of at least five separate measurements taken at random places on the surface of the specimens. All of the indentations were at least 5 mm away from the edges and from other indentations

4. Results and discussion

Preliminary study of room temperature creep of the material was carried out by testing the cast alloy under a constant load for different times. It was observed that the indentation length becomes larger with increasing loading time. The indentation creep data were measured at room temperature under constant loads of 20, 30, 50 and 100 N. The results are shown in Figs 1 and 2, where the indentation length is plotted against time. It can be seen from these figures that the indentation length increases with the loading time and the applied load.

The interesting feature of these figures is that in all four conditions of the material, the shape of the indentation curve is similar to that of an ordinary creep curve. The first stage of the curve records an increase in the concerned variable with time, with a decreasing rate, followed by a steady-state region where indentation sizes increase linearly with time. As the hardness test

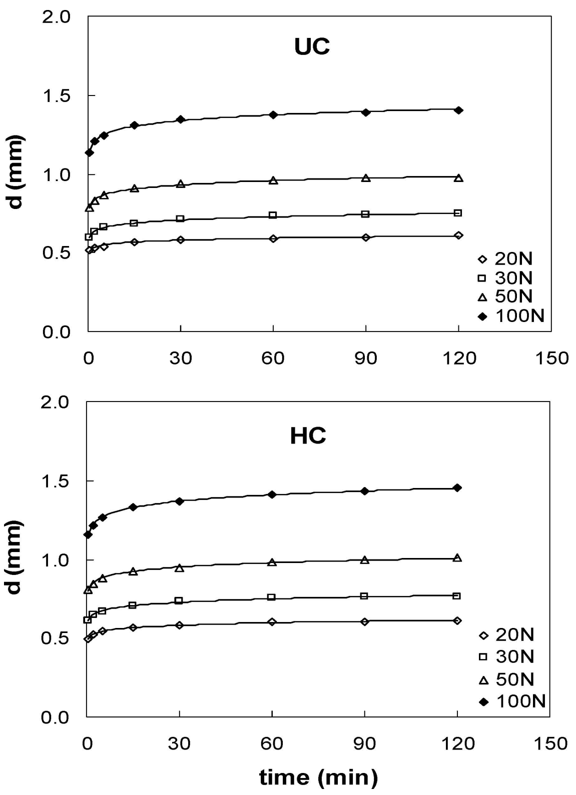

Figure 1 Indentation creep curves at different loads for the cast materials in the homogenized and unhomogenized conditions.

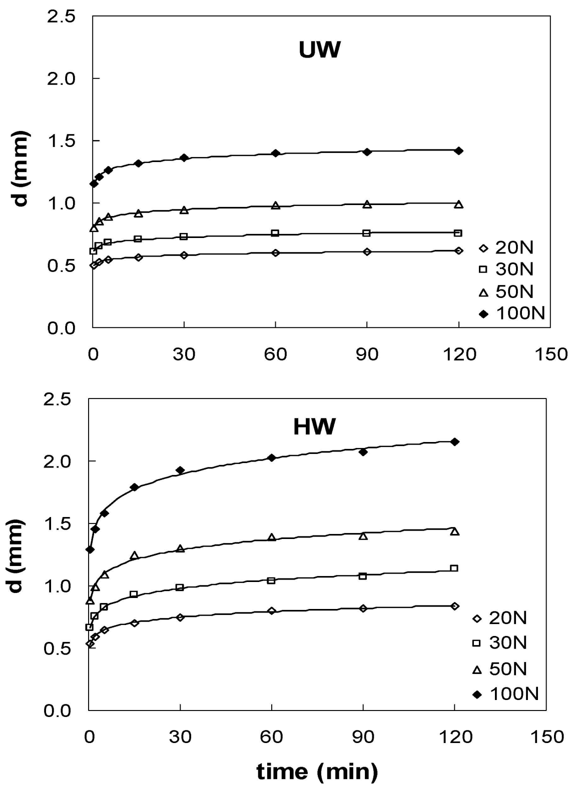

Figure 2 Indentation creep curves at different loads for the wrought materials in the homogenized and unhomogenized conditions.

is actually a compression test, fracture of the specimen dose not occur and hence it is obviously not possible to record a third stage of the curve as opposed to what happens in an ordinary creep test. It can be depicted from these figures that the level of indentation curves and their slopes in the steady-state region are higher for

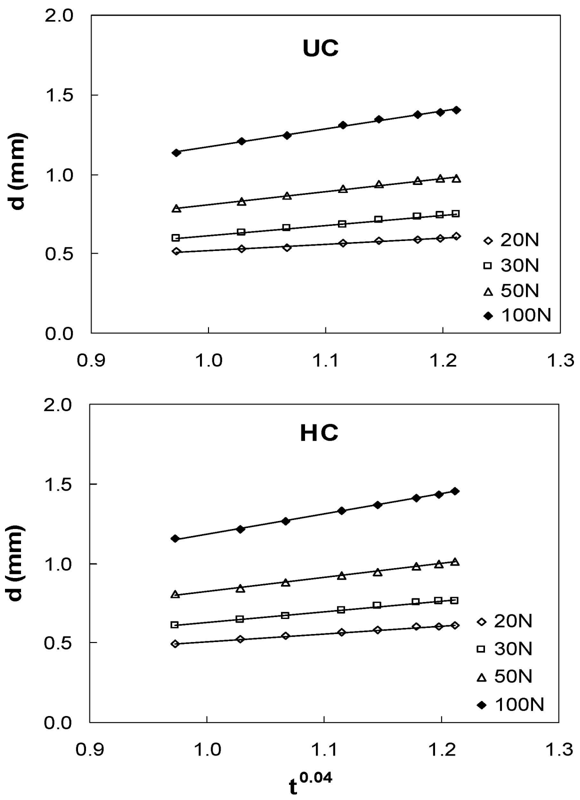

Figure 3 Indentation length as a function of $t^{0.04}$ for cast alloys at different loads.

the homogenized wrought (HW) condition. Other conditions, however, show very similar behaviors in terms of the level and slope of the indentation curves, implying that while indentation creep occurs more readily in the HW condition, there is not much difference in the indentation creep behavior of the UW, HC and UC conditions.

The indentation curves can be well represented by Equation 7. The validity of this equation is shown in Figs 3 and 4 for both cast and wrought alloys where the indentation length d is plotted against t^b. As can be seen, the measured points lie along straight lines for all different loading and material conditions. The power-law relationships for all different conditions of the material are given in Table I. It can be seen that for the homogenized wrought material the time exponent, b, is 0.10 while for all other conditions it is 0.04. Similar behavior has been reported by Roumina *et al.* [18], who obtained b values in the range of 0.02 to 0.09 for different cast and wrought Pb-Sb alloys. It should be noted that the time exponents b and therefore, the corresponding n values obtained from Equation 9, are materials' constants which depend on the structure and thus, are independent of the applied load. The correlation factors (R^2), greater than 0.99, indicate a very good linear fit of the data for all conditions

The stress exponent values obtained using Equation 9 and the data given in Figs 3 and 4 are shown in Table I. These exponents are 4.5 for the homogenized wrought material and 12 for other conditions. It is worth noting that the results of conventional creep tests on a cast and aged Sn-5.8%Sb alloy at room temperature are indicative of n values of 11.6 and 5.3 at high and

TABLE I Creep characteristics for different conditions of the material

Condition	Grain size (μm)	Load (N)	Relationship	R^2	Stress exponent (n)
Unhomogenized cast (UC)	35*	20	$d = 0.39t^{0.04} + 0.10$	0.976	12
		30	$d = 0.64t^{0.04} + 0.02$	0.997	
		50	$d = 0.82t^{0.04} + 0.01$	0.997	
		100	$d = 1.13t^{0.04} + 0.04$	0.995	
Homogenized cast (HC)	280	20	$d = 0.49t^{0.04} + 0.02$	0.995	12
		30	$d = 0.67t^{0.04} - 0.04$	0.993	
		50	$d = 0.86t^{0.04} - 0.04$	0.996	
		100	$d = 1.26t^{0.04} - 0.08$	0.999	
Unhomogenized wrought (UW)	60	20	$d = 0.49t^{0.04} + 0.02$	0.998	12
		30	$d = 0.64t^{0.04} - 0.01$	0.988	
		50	$d = 0.82t^{0.04} + 0.01$	0.996	
		100	$d = 1.17t^{0.04} + 0.01$	0.995	
Homogenized wrought (HW)	4.5	20	$d = 0.45t^{0.10} + 0.11$	0.999	4.5
		30	$d = 0.67t^{0.10} + 0.03$	0.996	
		50	$d = 0.83t^{0.10} + 0.11$	0.989	
		100	$d = 1.28t^{0.10} + 0.08$	0.996	

*Das.

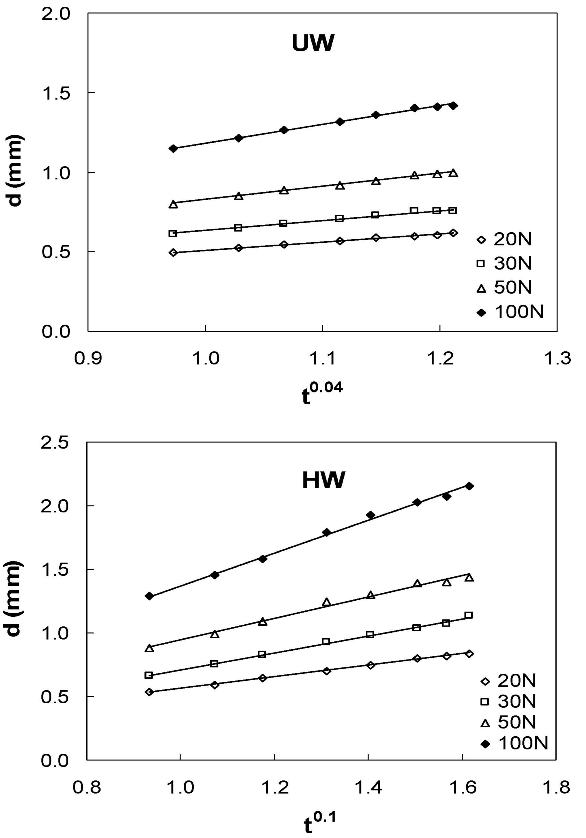

Figure 4 Indentation length as a function of $t^{0.04}$ and $t^{0.10}$ for wrought materials at different loads.

low stresses, respectively [3]. Other similar results obtained in the conventional and automated ball indentation (ABI) creep testing of rolled Sn-5%Sb sheets have yielded n values of about 5 at room temperature [1]. According to the power law creep, a decrease in stress exponent would result in an increase in the creep rate due to a decrease in yield strength [19]. Therefore, the homogenized wrought (HW) material with a lower n value is less resistant to indentation creep compared to the other conditions. The same result can also be extracted from the indentation curves shown in Figs 1 and 2, where, both the level of indentation curves and their slopes in the steady-state region are higher for this condition. In other conditions, however, there is not much increase in indentation length and in the steady-state region of indentation curves, the diagonal length only slightly increases with indentation dwell time. Therefore, steady-state creep rates for these conditions are expected to be much lower than those of the HW condition.

The observed difference in the indentation behavior of the cast and wrought alloys can be attributed to the microstructures of these materials. The microstructures of the cast and wrought materials are shown in Figs 5 and 6, respectively. It is observed that the UC

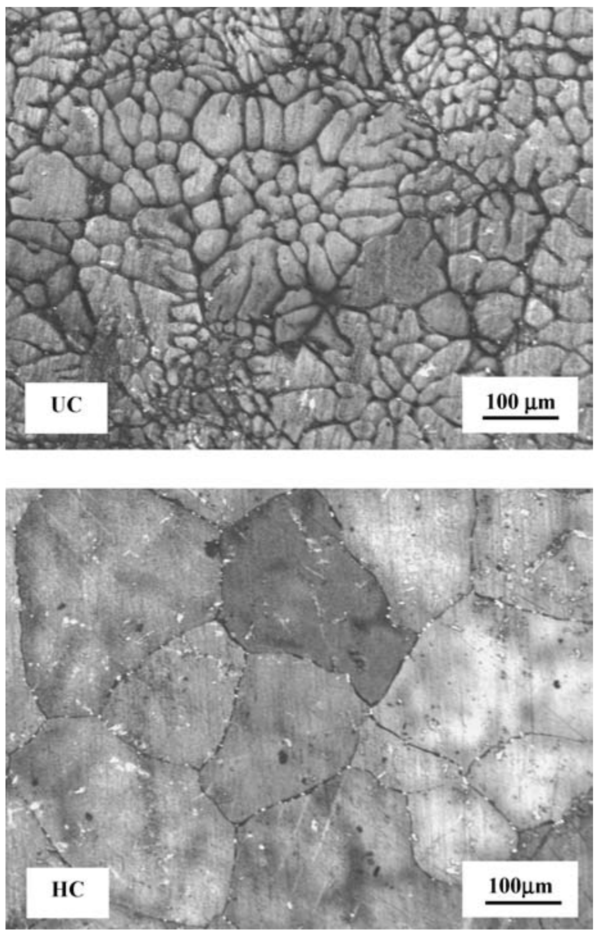

Figure 5 Optical microstructures of the cast materials in the unhomogenized and homogenized conditions.

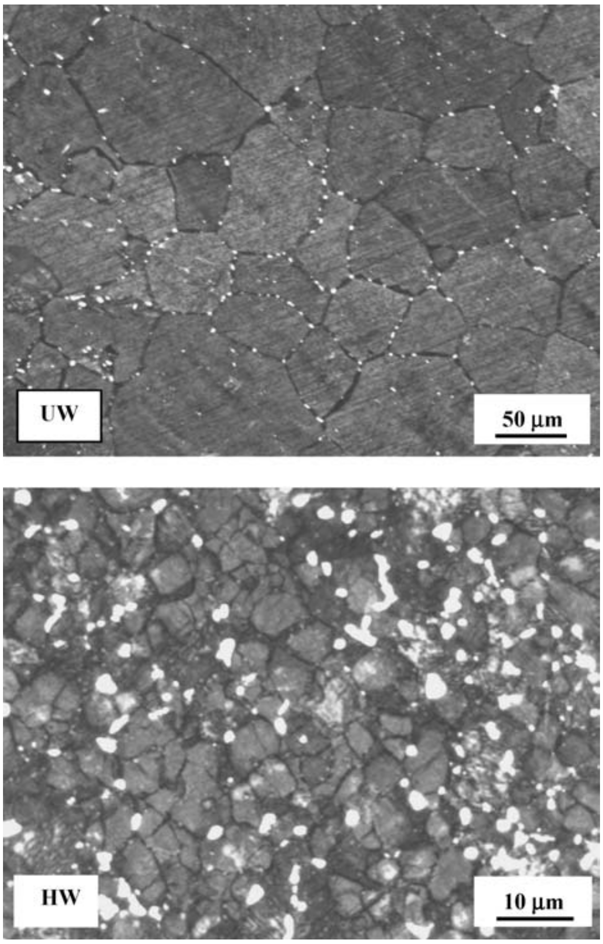

Figure 6 Optical microstructures of the wrought materials in the unhomogenized and homogenized conditions.

condition has a dendritic structure with a dendrite arm spacing (DAS) of about 35 μm. The HC material, however, has a rather coarse equiaxed grain structure with an average grain size of about 280 μm. This implies that the long time homogenization treatment has totally removed the dendritic structure, resulting in a recrystallized structure with little intermetallic particles at the grain boundaries. Both of the wrought conditions have equiaxed grain structures with different grain sizes of 60 and 4.5 μm for the UW and HW conditions, respectively. It seems that homogenization of the cast material followed by cold rolling, provides sufficient driving force for precipitation of the second phase particles and a complete recrystallization of the material. The high volume fraction of the particles in the HW condition is in sharp contrast with those of the other conditions. It seems that the high volume fraction of second phase particles together with the very fine grain size has resulted in a higher creep rate under testing conditions.

It is believed that under the experimental conditions where the power law creep relation is valid, the value of stress exponent can be related to the mechanisms controlling the deformation process. However, it should be cautioned that making mere comparisons of the stress exponents, without additional information on activation energies, does not provide sufficient information to draw insightful comparisons on creep mechanisms of materials. In fact, deformation of polycrystalline materials at temperatures above $0.5T_m$ can take place by different deformation mechanisms, associated with different stress exponent values. It is reported that diffusional creep is associated with n values around 1 [16], grain boundary sliding leads to n values close to 2 [19], dislocation climb is responsible for n values in the 4–6 range [12]. Mechanisms associated with dislocation movement such as dislocation creep are attributed to $n > 6$ [11]. In the present investigation, although the structure of the UC, HC and UW conditions are totally different in terms of grain size and second phase volume fraction, they all exhibit the same stress exponent implying that their creep mechanism is structure-independent. The high stress exponent of about 12 in these conditions may lead us to the conclusion that the dislocation creep might be the dominant mechanism. For the HW condition, however, the n value of about 5 together with the very fine grain structure and a high volume fraction of second phase particles suggest that dislocation climb could be the creep mechanism.

5. Conclusions

(1) The indentation creep tests performed at room temperature on cast and wrought Sn-5%Sb alloys showed that an indentation creep process occurs in these alloys. It is further demonstrated that indentation creep test is capable of evaluating creep behavior of materials using small specimens

(2) The data analyses showed that the simple theory, based on steady-state power-law creep equation, has the capacity to describe the indentation creep data satisfactorily. In all conditions of the material, the stress exponent values are independent of the loading conditions in hardness tests.

(3) The indentation creep process can be characterized by the stress exponents. The stress exponents obtained from indentation curves were found to be 4.5 for the HW and 12 for all other conditions. This implies that dislocation climb could be the dominant mechanism in creep of the former material while in all other conditions dislocation creep is the possible creep mechanism.

Acknowledgments

The authors thank the Research Council of Tehran University for providing financial support of this work under Grant No. 615/1/798.

References

1. K. L. MURTY, F. M. HAGGAG and R. K. MAHIDHARA, *J. Elec. Mater.* **26** (1997) 839.
2. P. T. PIANCO and D. R. FREAR, *JOM* **45** (1993) 14.
3. R. J. MCCABE and M. E. FINE, *Met. Mater. Trans.* **33A** (2002) 1531.
4. H. MAVOORI, *JOM* **52** (2000) 29.
5. R. J. MCCABE and M. E. FINE, *J. Elec. Mater.* **31** (2002) 1276.
6. N. WADE, K. WU, J. KUNI, S. YAMADA and K. MIYAHARA, *J. Elec. Mater.* 30 (2001) 1228.
7. M. FUJIWARA and M. OTSUKA, *Mater. Sci. Eng.* A **319–321** (2001) 929.
8. R. MAHMUDI, R. ROUMINA and B. RAEISINIA, *ibid.* A **382** (2004) 15.

9. R. ROUMINA, B. RAEISINIA and R. MAHMUDI, *Scripta Mater.* **51** (2004) 497.
10. T. R. G. KUTTY, C. GANGULY and D. H. SASTRY, *ibid.* **34** (1996) 1833.
11. A. DE LA TORRE, P. ADEVA and M. ABALLE, *J. Mater. Sci.* **26** (1991) 4351.
12. G. SHARMA, R. V. RAMANUJAN, T. R. G. KUTTY and G. P. TIWARI, *Mater. Sci. Eng.* A **278** (2000) 106.
13. G. CSEH, N. Q. CHINH, P. TASNADI and A. JUHASZ, *J. Mater. Sci.* **32** (1997) 5107.
14. P. M. SARGENT and M. F. ASHBY, *Mater. Sci. Tech.* **8** (1992) 594.
15. B. N. LUCAS and W. C. OLIVER, *Metall. Mater. Trans.* **30A** (1999) 601.
16. T. G. LANGDON, *Mater. Sci. Eng.* A **283** (2000) 266.
17. T. O. MULHEARN and D. TABOR, *J. Inst. Metal.* **89** (1960) 7.
18. R. ROUMINA, B. RAEISINIA and R. MAHMUDI, *J. Mater. Sci. Letts.* **22** (2003) 1435.
19. B. WALSER and O. D. SHERBY, *Scripta Metall.* **16** (1982) 213.

Received 28 November 2004
and accepted 31 January 2005